Oblique-Incidence Reflectivity Difference and Fluorescence Imaging of Oligonucleotide and IgG Protein Microarrays

James P. Landry[1], X. D. Zhu[1], X. W. Guo[1], and J. P. Gregg[2]
[1]Department of Physics, University of California at Davis
One Shields Avenue, Davis, CA 95616
[2]Department of Molecular Pathology, University of California at Davis, Sacramento, CA

ABSTRACT

We have constructed an oblique-incidence reflectivity difference (OI-RD) microscope for fluorescent label-free imaging of DNA and protein microarrays on standard glass substrates. Using both OI-RD and fluorescence images, we demonstrate a difference in wetting behavior of labeled and unlabeled IgG protein molecules deposited on an aldehyde-derivatized glass surface. The potential of fluorescent labeling agents to influence the properties of proteins highlights the need for label-free microarray detection techniques to supplement existing fluorescence methods. We also present OI-RD images of an oligonucleotide microarray after printing and washing procedures to demonstrate the use of OI-RD for non-destructive monitoring of changes in the optical properties of microarrays during processing.

INTRODUCTION

Microarrays are microscopic spots of biomolecules (such as DNA or protein) arranged in a regular pattern and immobilized on a solid substrate (typically glass) [1]. Due to their inherent high spot density, microarrays enable thousands of biomolecular interactions to be investigated in a parallel fashion, typically using fluorescent probe molecules and confocal fluorescence microscopy. In this paper, we introduce *oblique-incidence reflectivity difference* (OI-RD) microscopy as a label-free optical method for the detection of microarrays on standard substrates, such as glass. In contrast to other label-free optical methods, like surface plasmon resonance or waveguide techniques, OI-RD does not require a special substrate material or sample geometry. We will present fluorescence and OI-RD images of immunoglobulin-G (IgG) protein microarrays showing a difference in wetting behavior of labeled and unlabeled protein. The potential of fluorescent labeling agents to influence the properties of proteins highlights the need for label-free protein microarray [2] detection techniques to supplement existing fluorescence methods. Finally, we will demonstrate the use of OI-RD to quantitatively monitor the optical properties of microarrays without fluorescent labeling using the printing and washing of oligonucleotide microarrays as an example.

INSTRUMENT

OI-RD is a particular form of optical ellipsometry used to directly measure small changes in optical properties of thin films [3-6]. At an oblique angle of incidence, the p-polarized and s-polarized surface reflectivities change differently as the thickness and/or complex dielectric constant of a deposited film change. OI-RD directly measures the real and imaginary parts of the differential ellipsometric ratio, defined as

$$\frac{\delta\rho}{\rho_\circ} = \left[\frac{|r_p| - |r_{p_\circ}|}{|r_{p_\circ}|} - \frac{|r_s| - |r_{s_\circ}|}{|r_{s_\circ}|} \right] + i\left[\left(\phi_p - \phi_{p_\circ}\right) - \left(\phi_s - \phi_{s_\circ}\right) \right] \quad (1)$$

where $r_p = |r_p| e^{i\phi_p}$ is the p-polarized reflectivity, $r_s = |r_s| e^{i\phi_s}$ is the s-polarized reflectivity, and $r_{p_\circ}$ and $r_{s_\circ}$ denote the reflectivities of the bare substrate before a film is deposited. It can be shown that the real and imaginary parts of the differential ellipsometric ratio are proportional to the changes in the standard ellipsometric angles ψ and Δ, respectively [6]. When small changes in the ellipsometric angles are of primary interest, OI-RD gives improved signal-to-noise ratio by directly measuring these changes instead of subtracting two large angles.

The optical layout of the OI-RD microscope constructed for this study is illustrated in Figure 1. A polarized He-Ne laser beam (λ = 632 nm) passes through a polarization modulator (PEM-90, Hinds Instruments), causing the polarization state to oscillate between s and p-states at a frequency Ω = 50 kHz (with elliptical intermediate states). The Pockels cell introduces an adjustable phase difference between the s and p-polarization components. The beam is focused on the surface (spot diameter ~ 3 μm) and reflected at an oblique angle of incidence (θ = 45°). The beam then passes through a rotatable analyzer, converting the oscillating polarization into an oscillating intensity that is Fourier analyzed with lock-in amplifiers (SR850, Stanford Research Systems). The analyzer and Pockels cell are adjusted to zero the first and second harmonic intensity components when the beam is reflected from the bare substrate. Images of the reflectivity differences of deposited biomolecular films are generated by translating the microarray under the fixed optics and recording the first and second harmonic components of the intensity (proportional to the imaginary and real parts of the differential ellipsometric ratio, respectively).

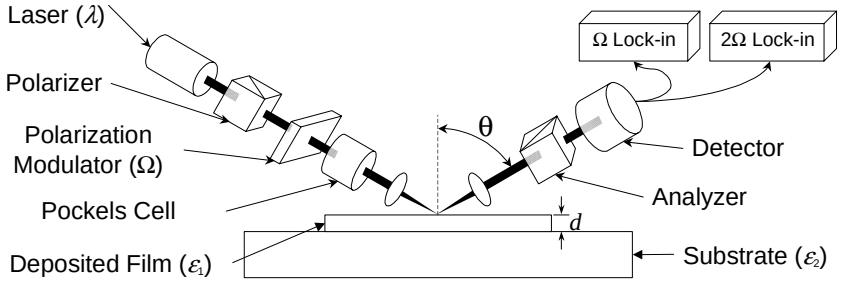

Figure 1. Optical layout of the OI-RD microscope.

For the case of ultrathin films of thickness d such that $d/\lambda << 1$, it can be shown that the differential ellipsometric ratio can be written as

$$\frac{\delta\rho}{\rho_o} \approx i\left[4\pi \frac{\varepsilon_2}{(\varepsilon_2 - 1)} \frac{\sin^2\theta}{\cos\theta\left(\varepsilon_2 - \tan^2\theta\right)} \right] \frac{(\varepsilon_2 - \varepsilon_1)(\varepsilon_1 - 1)}{\varepsilon_1} \left(\frac{d}{\lambda}\right) \quad (2)$$

where θ is the angle of incidence, ε_1 is the dielectric constant of the deposited film layer, and ε_2 is the dielectric constant of the substrate [3]. Molecular properties of the film, such as volume

density and molecular polarizability, are embedded in the dielectric constant ε_1. For the transparent glass substrates and transparent protein and DNA films studied here, only $\mathrm{Im}\{\delta\rho/\rho_\circ\}$ is non-zero, so we will focus on it for the remainder of this paper. In this study, with $\theta = 45°$ and $\varepsilon_2 = 2.31$, the factor in square brackets has a value of 12.0.

EXPERIMENTAL DETAILS

The IgG protein microarrays were created using a GMS 417 pin-and-ring contact printing robot. The pin diameter was 125 μm and the volume of solution deposited was about 1 nL. Unlabeled, Cy3 labeled, and Cy5 labeled whole IgG monoclonal antibodies were purchased (Jackson Immuno Research) in lyophilized form and resuspended in 1×PBS solution. Spectrophotometric measurements of the nominally labeled IgG solutions yielded a dye-to-protein ratio of ~0.5, indicating that about half of the IgG in the solution was actually unlabeled. The dye-to-protein ratio was computed by measuring the absorbance of the protein at λ = 280 nm and the absorbance of the dye at the excitation peak of the dye (λ = 550 nm for Cy3, λ = 650 nm for Cy5) [8]. The protein was suspended in a 40% glycerol, 60% 1×PBS (v/v) printing solution, diluted to a series of concentrations with 1×PBS, and then printed on aldehyde-derivatized glass slides (CEL Associates). The IgG is covalently bound to the substrate through a Schiff base linkage formed through nucleophilic attack of the surface aldehyde groups by the primary amines of lysine residues on the surface of the IgG molecule. Excess printed protein was washed off by immersing in ddH_2O for 1 hour followed by spin-drying in a centrifuge. For reaction with a secondary antibody, the microarray was first blocked by immersing in a 1% solution of BSA in 1×PBS for 1 hr. The secondary antibody was mixed in a 1% BSA solution, pipetted into a reaction chamber (Grace Biolabs) placed over the microarray, and then allowed to incubate at room temperature for 30 minutes. After the reaction, the microarray was rinsed in 0.1% TWEEN20 in 1×PBS, then in 1×PBS, and finally in ddH_2O and then spun dry. Cy5 and Cy3 fluorescence images were acquired with a GMS 418 confocal fluorescence scanner.

The oligonucleotide microarrays were created using the same contact printing robot as the IgG microarrays. Custom 60-base long single-stranded oligonucleotides were purchased (Sigma-Genosys and QIAGEN-Operon) in lyophilized form and then resuspended and diluted to a series of concentrations in nuclease-free ultra-pure water. The oligonucleotides were printed on poly-L-lysine coated glass slides (CEL Associates). The deposited oligonucleotides are electrostatically bound to the substrate since at neutral pH the amino groups of the poly-L-lysine film are positively charged while the sugar-phosphate backbones of the oligonucleotides are negatively charged. Furthermore, covalent bonds between the surface amines and thymine bases in the oligonucleotides were induced by irradiating with UV light (λ = 254 nm) at a dosage of 60 mJ/cm^2 after printing. Excess printed oligonucleotide was washed off by immersing in sodium borate buffer (pH 8.0) for 10 minutes followed by spin-drying in a centrifuge.

RESULTS AND DISCUSSION

IgG Protein Microarrays

Figure 2(a) is an OI-RD image of $\mathrm{Im}\{\delta\rho/\rho_\circ\}$ for an IgG protein microarray printed on aldehyde-derivatized glass and Figure 2(b) is a corresponding two-color fluorescence image.

Rabbit, mouse, and human IgG solutions were printed in a series of concentrations. The nominally labeled IgG solutions were actually a mixture of labeled and unlabeled IgG. The images in Figures 2(a) and 2(b) were acquired after removing excess printed protein as described previously. The OI-RD image shows both the labeled and unlabeled IgG films covering the printed spots. However, the fluorescence image reveals that the Cy5 and Cy3 labeled IgG proteins tend to aggregate together, in this case on the edge of the printed spot. Since the OI-RD image reveals the presence of a film in the center of these spots, we conclude that the unlabeled IgG printed on these same spots has spread over the spot. This phase segregation is likely due to a difference in hydrophobicity of the labeled and unlabeled proteins due to the hydrophobic cyanine dyes. Solid printing pins have a tendency to remove liquid from the center of the deposited droplet during the upstroke of the pin [1]. These images show that the labeled IgG molecules remain on the edge of the spot while the unlabeled IgG wets the entire spot.

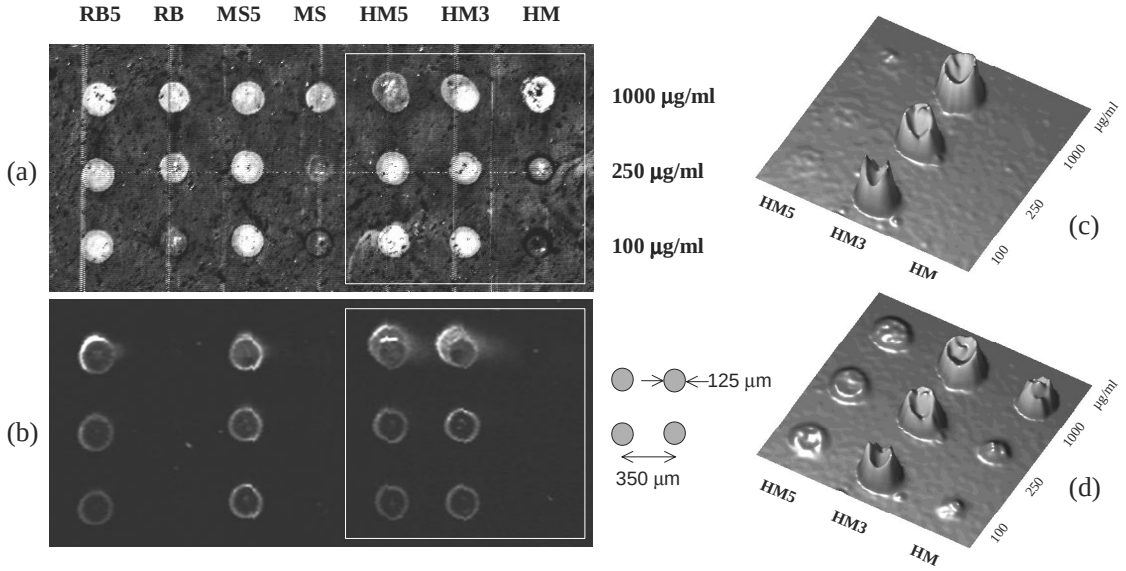

Figure 2. (a) OI-RD image of $\mathrm{Im}\{\delta\rho/\rho_\circ\}$ for an IgG protein microarray. Feature sizes are indicated. Rabbit IgG (RB), Cy5 labeled rabbit IgG (RB5), mouse IgG (MS), Cy5 labeled mouse IgG (MS5), human IgG (HM), Cy3 labeled human IgG (HM3), and Cy5 labeled human IgG (HM5) were printed in a series of concentrations (listed on the right). **(b)** Combined Cy3 and Cy5 fluorescence image of the IgG microarray. Cy3 fluorescence images of region of interest (boxed in (a) and (b)) before reaction **(c)** and after reaction **(d)** with Cy3 labeled goat anti-human secondary antibody. The vertical scales in (c) and (d) are identical.

To confirm this scenario, we blocked the remaining aldehyde groups with IgG-free bovine serum albumin (as described above) and then reacted the microarray with a Cy3 labeled goat anti-human secondary antibody. The region of interest for the reaction is boxed in Figures 2(a) and 2(b). Cy3 fluorescence images of the region of interest before and after reaction with the fluorescent secondary antibody are given in Figures 2(c) and 2(d). The reaction with the HM column revealed that the unlabeled human IgG covered the entire spot and did not aggregate on the edge. The reaction with the HM5 column showed that the secondary antibody reacted with the labeled IgG on the edge of the spot and with unlabeled IgG in the center of the spot, consistent with the OI-RD image. The HM3 column showed a decrease in average fluorescence

intensity (even after accounting for the small amount of photobleaching due to the scanner) indicating that IgG desorbed from the surface during the reaction or subsequent washing steps. However, the ratio of the minimum fluorescence intensity of the center of the HM3 spots and the maximum intensity of the edge of the HM3 spots decreased by 12% on average after the reaction with the secondary antibody, indicating binding of the Cy3 labeled secondary antibody to IgG in the center of the HM3 spots.

Oligonucleotide Microarrays

OI-RD can be used to monitor changes in the optical properties of a microarray during processing without the need for fluorescent labels, staining, or test reactions. This is demonstrated for the printing and washing procedures of a 60-mer oligonucleotide microarray in Figure 3. After printing and UV cross-linking, for sufficiently high concentrations, the OI-RD signal increases linearly with printing concentration. This corresponds to an increase in the film thickness as unbound DNA is piled up on the spot. After the washing step, the OI-RD signal levels off for all spots printed with concentrations in excess of 50 µM. This level corresponds to a remaining stably bound DNA monolayer saturating the surface binding sites. Assuming these spots have a thickness of 1 nm [9], Equation 2 gives a dielectric constant of $\varepsilon_1 = 2.12$ for the oligonucleotide film, in good agreement with a previously reported value of 2.14 [10]. The thickness of the DNA films after printing can be calculated using this dielectric constant and Equation 2, assuming the DNA remains densely packed as it is piled on the spot. Doing so gives a maximum thickness of 6.4 nm for the 300 µM spot. Furthermore, the OI-RD signal rolls off to zero for low concentrations since they yield sub-monolayer coverage resulting in smaller effective dielectric constants, eventually reaching a value of $\varepsilon_1 = 1$ at zero concentration.

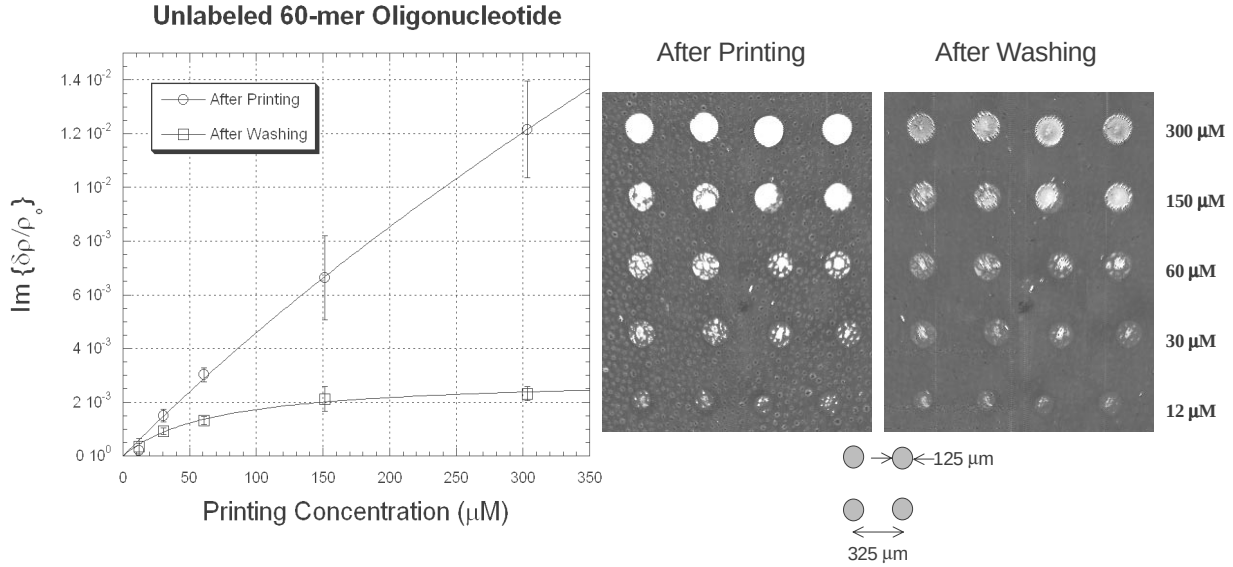

Figure 3. On the right are OI-RD images of an unlabeled oligonucleotide in quadruplicate (printed in a series of concentrations listed on the right) taken after printing and washing. Feature sizes are indicated. The plot on the left shows the average OI-RD $\mathrm{Im}\{\delta\rho/\rho_\circ\}$ value of the spots versus the printing concentration for each process. The error bars are the standard deviations of the four replicates. The lines are guides for the eyes.

The data in Figure 3 show that OI-RD can be used to gauge the quantity of deposited oligonucleotides. This was corroborated by imaging Cy5 labeled oligonucleotides, which exhibited a linear relation between the average OI-RD signal and average fluorescence intensity of the spots after printing and after washing. This indicates that OI-RD could be used to account for fluctuations of the fluorescence intensities of spots on a microarray after a hybridization reaction due to variations in the quantity of deposited oligonucleotide.

CONCLUSION

We have introduced OI-RD microscopy as a label-free optical technique for imaging microarrays on standard glass substrates. OI-RD and fluorescence microscopy were used together to demonstrate a difference in wetting behavior of labeled and unlabeled IgG proteins printed on the same spot on an aldehyde-functional substrate. This example illustrates the possibility of fluorescent labeling agents altering the physical and chemical properties of proteins, suggesting a need for label-free microarray detection methods, such as OI-RD, to supplement fluorescence-based protein microarray assays. Furthermore, OI-RD can be used as a non-invasive quality control for standard microarray procedures such as printing and washing or to gauge the density of deposited films in order to normalize fluorescence images of reacted microarrays. Moreover, with properly optimized protocols, it should be possible to use OI-RD to observe specific binding to spots on microarrays without the use of fluorescent labels.

REFERENCES

1. Mark Schena, *Microarray Analysis*. (John Wiley and Sons, Hoboken, 2003) pp. 1-17, p. 184.
2. G. MacBeath and S. L. Schreiber, Science **289**, 1760 (2000).
3. A. Wong and X. D. Zhu, Appl. Phys. A **63**, 1 (1996).
4. X. D. Zhu, H. B. Lu, Yang Guo-Zhen, Li Zhi-Yuan, Gu Ben-Yuan, Zhang Dao-Zhong, Phys. Rev. B **57,** 2514 (1998).
5. X. D. Zhu, Si Weidong, X. X. Xi, Jiang Qidu, Appl. Phys. Lett. **78**, 460 (2001).
6. W. Schwarzacher, J. Gray, X. D. Zhu, Electrochemical and Solid-State Lett. **6**, C73 (2003).
7. R. M. A. Azzam and N. M. Bashara, *Ellipsometry and Polarized Light*. (Elsevier Science, New York, 1987) p. 305.
8. H. J. Gruber, C. D. Hahn, G. Kada, C. K. Riener, G. S. Harms, W. Ahrer, T. G. Dax, H. G. Knaus, Bioconjugate Chem. **11**, 696 (2000).
9. S. V. Lemeshko, T. Powdrill, Y. Y. Belosludtsev, M. Hogan, Nucleic Acids Res. **29**, 3051 (2001).
10. D. E. Gray, S. C. Case-Green, T. S. Fell, P. J. Dobson, E. M. Southern, Langmuir **13**, 2833 (1997).